Supersensitizing Dyes

DOI: 10.1002/ange.200500363

Supermolecular Control of Charge Transfer in Dye-Sensitized Nanocrystalline TiO_2 Films: Towards a Quantitative Structure–Function Relationship**

Saif A. Haque, Samantha Handa, Katja Peter, Emilio Palomares, Mukundan Thelakkat, and James R. Durrant*

The attachment of redox or photoactive molecules to solid surfaces is important for the development of many applications. One area of research that is receiving extensive interest at present is the immobilization of molecular dyes on mesoporous nanocrystalline metal oxide electrodes. Such functionalized films are currently under investigation for device applications ranging from solar cells to chemical and biological sensors.[1–6] Recently there has been interest in the use of more complex supramolecular or multifunctional sensitizers to build a range of new applications including heterosupramolecular devices.[7–14] The use of such materials is particularly attractive as it enables the development of electroactive structures that exhibit a remarkable degree of structural organization, improved stability, redox reversibility, and a greater functional diversity.[14–16] A key requirement for the exploitation of such materials in electronic devices is the ability to electrically interface the supramolecular or multifunctional materials to the metal oxide electrode whilst achieving control over key device parameters such as interfacial charge transfer. Such issues have been considered in great detail for molecular-based adsorbates,[17] but are yet to be addressed systematically for functionalized films that comprise more complex, supramolecular or multifunctional sensitizer dyes. This understanding is both of fundamental interest and essential to the design and application of such materials in electronic devices. Herein we address this issue by exploring a class of multifunctional sensitizer dyes that exhibit multistep charge-transfer cascades. We show that by careful design of the "supersensitizer" dye it is possible to modulate the charge-recombination dynamics by five orders of magnitude and achieve remarkably long-lived photoinduced charge separation at a dye/TiO_2 interface. These studies enable us to address the relationship between supermolecular dye structure and interfacial charge transfer and provide an insight into the fundamental processes that govern charge-transfer dynamics at the supermolecular sensitizer dye/TiO_2 interface.

We have used sensitizer dyes in which the dye chromophore is modified by the covalent attachment of secondary electron donors. By introducing such secondary electron-transfer cascades within the dye structure, as illustrated in Figure 1, it is possible to retard the charge-recombination dynamics by increasing the physical separation between the dye–cation moiety and the surface of the TiO_2 surface. Such an approach has been recently adopted, however in all cases reported to date, only simple monomeric electron-donor groups have been employed.[9,14,18] Herein we consider the influence of structure of the electron-donating moiety upon the charge-recombination dynamics. In particular we address the influence of extended π-conjugation within the electron-transfer cascade and the use of polymeric electron-donating units which allows us to address the relationship between supermolecular dye structure and interfacial charge-transfer dynamics. Density functional theory (DFT) ab initio calculations are performed to determine the spatial distribution of the HOMO orbitals of the dyes. These slow charge-recombination dynamics observed herein are shown to be consistent with the increased physical separation of the HOMO orbitals of dye molecules from the TiO_2 surface as indicated by the DFT calculations.

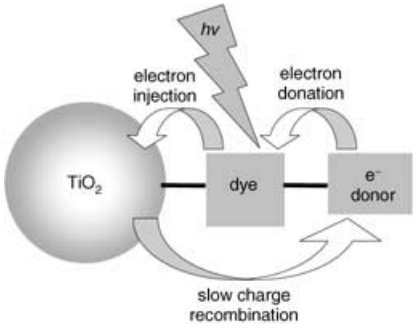

Figure 1. The heterosupermolecular structure and the charge-transfer processes occurring at the dye/TiO_2 interface.

We have employed three bifunctional dyes that differ in the structure of electron-donor component (Scheme 1). Our dyes are built with carboxylated ruthenium (II) polypyridyl chromophores and carry aromatic-amine-based electron-donor groups attached on the 4 and 4′ positions of the bipyridyl (bpy) ligand. Such electron-donor groups are ideal

[*] Dr. S. A. Haque, S. Handa, Dr. J. R. Durrant
Centre for Electronic Materials and Devices
Department of Chemistry
Imperial College of Science Technology and Medicine
London SW72AZ (UK)
Fax: (+44) 207-594-5801
E-mail: s.a.haque@imperial.ac.uk
Dr. E. Palomares
Institut de Ciencia Molecular (IcMol)
Universitat de Valencia
461000 Burjassot, Valencia (Spain)
K. Peter, Dr. M. Thelakkat
Makromoleculare Chemie 1
Universitat Bayreuth
95440 Bayreuth (Germany)

[**] We thank the Engineering and Physical Sciences Research Council (EPSRC), BP Solar Ltd, and the European Commission (project 'Molycell, SE56-CT-2003-502783) for financial support. M.T. would like to thank Deutsche Forschungsgemeinschaft (SFB 481 project B4) for the financial support. We would also like to thank Dr. Ian Gould for help with the Gaussian HOMO orbital calculations.

Supporting information for this article is available on the WWW under http://www.angewandte.org or from the author.

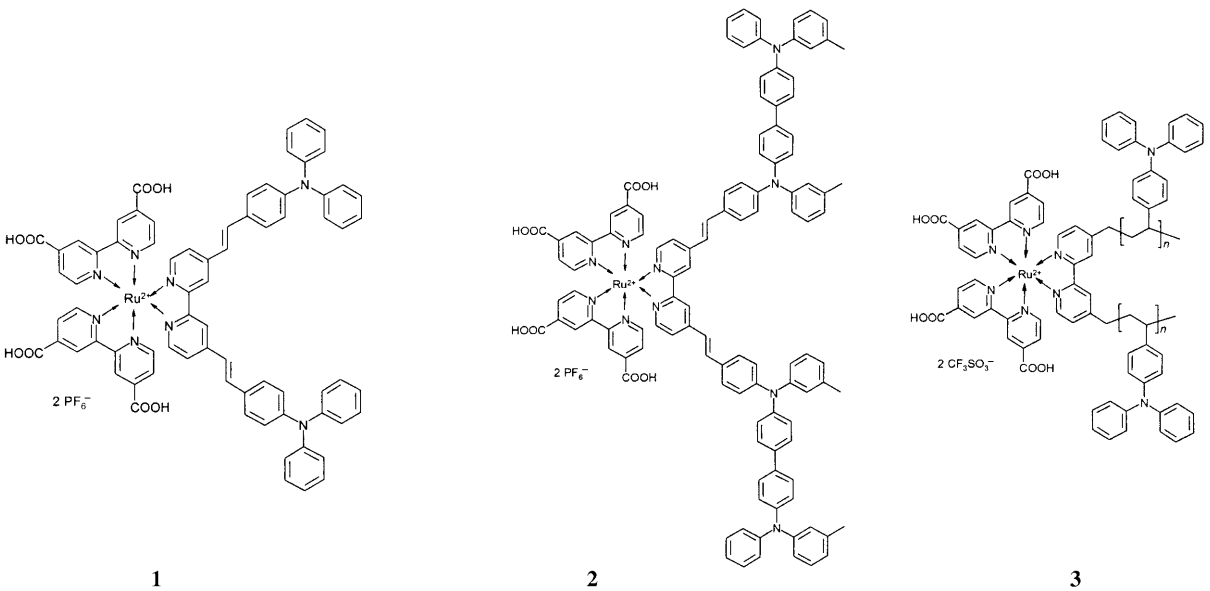

1 2 3

Scheme 1. The structure of the three dyes employed in this study [Ru^{II}(dcbpy)$_2$(TPAbpy)] (**1**), [Ru^{II}(dcbpy)$_2$(TPDbpy)] (**2**), and [Ru^{II}(dcbpy)$_2$(poly-TPAbpy)] (**3**); dc = dicarboxylate.

for this purpose as they possess low ionization potentials which facilitate the formation of cation radicals, thereby allowing multistep charge transfers. Dyes **1** and **2** comprise low-molecular-weight electron-donating units, namely, triphenylamine (TPA) and *N*,*N*′-diphenyl-*N*,*N*′-bis(3-methylphenyl)-[1,1′-biphenyl]-4,4′-diamine (TPD), respectively. Dye **3** comprises of poly(vinyl triphenylamine) chains (poly-TPA) with approximately 100 repeat units attached to one of the bipyridine units of the Ru^{II} core.[19] Details of the synthesis of these dyes and characterization are provided in the Supporting Information. The attachment of the dyes to the nanocrystalline TiO_2 films was achieved by immersion of the preformed metal oxide electrodes in solutions of the dyes at 25 °C, for 2 h for dyes **1** and **2** and overnight for dye **3**. All three dyes incorporate carboxylate groups (-COOH) to achieve direct binding to the TiO_2 surface. All three dyes were found to result in strong adsorption to the surface of the electrode.

Transient absorption spectroscopy was employed to monitor the charge-recombination dynamics following photo-excitation of the dye. Details of the transient absorption apparatus have been described previously.[20–22] The dye-sensitized films were incorporated into a sealed glass cell and degassed with argon gas prior to transient absorption studies to ensure an anaerobic environment. Experiments employed low excitation energy densities ($\approx$25 μJ cm^{-2} at 430 nm for all three dyes), these excitation densities being selected to ensure matched densities of absorbed photons for the three dyes, this corresponding to approximately 0.5 injected electron per TiO_2 particle.

The recombination dynamics were monitored by observing the decay of the photoinduced cation absorption of the three dyes. Typical data for the dyes are shown in Figure 2 employing a probe wavelength of 850 nm for all three dye/TiO_2 film combinations. The transient absorption traces

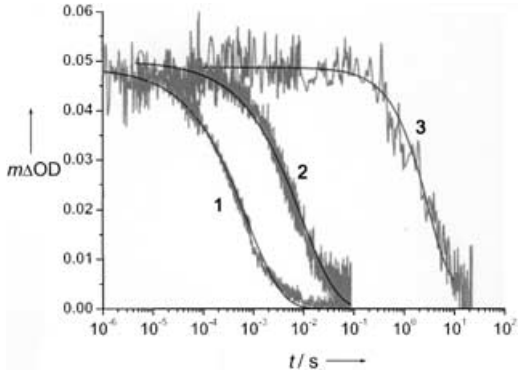

Figure 2. Transient absorption data obtained for nanocrystalline TiO_2 films sensitized with dyes **1**–**3**. The decay kinetics are assigned to the charge recombination of the photo-generated dye cations with the electrons in the TiO_2 [Eq. (2)]. The black lines indicate the fit, see text for details.

shown in Figure 2 follow the formation of the supermolecular-dye cations [Eq. (1)] and their recombination with photo-injected electrons [Eq. (2)].

$$\mathrm{Dye} \xrightarrow{h\nu} \mathrm{Dye}^* \rightarrow \mathrm{Dye}^+ + e^-_{TiO_2} \quad (1)$$

$$\mathrm{Dye}^+ + e^-_{TiO_2} \rightarrow \mathrm{Dye} \quad (2)$$

The absence of any grow-in of the transient signal is indicative that both the electron injection and arylamine oxidation by the $\{Ru(bpy)_3\}^{3+}$ component of the dye occurs within the time resolution of our apparatus; this result is consistent with previous studies.[23–26] However it is apparent that the recombination dynamics observed for all three dyes differ significantly, with dyes **1**, **2**, and **3** exhibiting recombination half-times ($t_{50\%}$) of 350 μs, 5 ms, and 4 s, respectively. It

is noteworthy that dye **3**/TiO_2 combination exhibits the longest lifetime reported to date for a dye-sensitized metal oxide film.

We attribute the retardation of the charge recombination observed for dyes **2** and **3** to an increase in the physical separation of dye cation from the metal oxide surface as a result of the multistep translation of the oxidized moiety away from the TiO_2 surface. To support this argument we have performed DFT ab initio calculations to determine the spatial distribution of the HOMO orbitals of **1**–**3**. These calculations were carried out using the Gaussian visualizer with a Gaussian View 3.08 program running on an AMD Athlon 64-bit processor computer. The DFT calculations employed Becke's (B3) three parameter hybrid functional with (LYP) correlation functional (B3LYP). The electronic structures of the complexes were determined using a general basis set with 6-31G(d) for nitrogen, oxygen, and carbon atoms, 6-31G for hydrogen atoms, and an effective core potential basis set LANL2DZ for the ruthenium atoms, full details of which are given in the Supporting Information. The HOMO orbital profiles for the three dyes are shown in Figure 3. The HOMO distribution in $[Ru^{II}(dcbpy)_3]$ dyes without any electron donating groups are centered entirely at the ruthenium core and not on the ligands. However, the HOMO orbitals of **1** are delocalized partially over the bipyridyl group and TPA units.

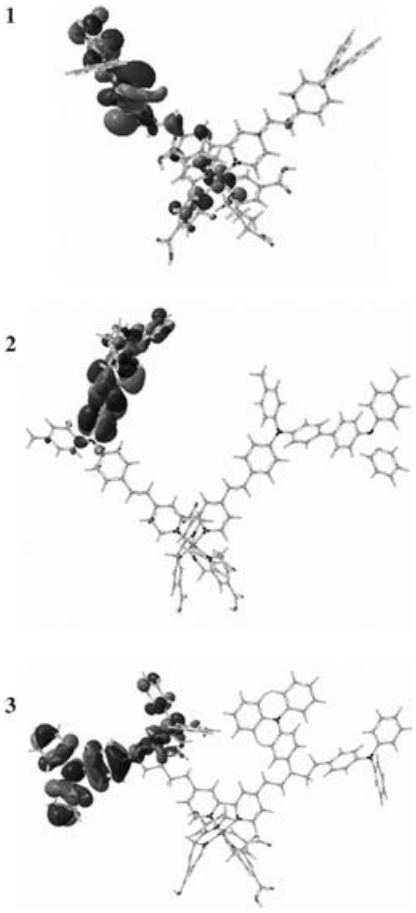

Figure 3. Graphical representation of the HOMOs of dyes **1**–**3** as determined from DFT ab initio calculations.

In contrast, for **2** and **3** the HOMO orbitals are located only on the phenylamine moieties, resulting in an increased separation of the HOMO orbitals from the TiO_2 surface compared to dye **1**. The approximate distances of the excited-state HOMO from the TiO_2 surface, as obtained from these calculations, were 10.8 Å for **1**, 15.6 Å for **2**, and 16.7 Å for **3**.[26] These calculations were complimented by cyclic voltammetry (CV) measurements which indicate a translation of the oxidizing moiety onto the aryl-amine components of the dye and thus further away from the surface of the TiO_2, resulting in an increased physical separation; this result is in agreement with previous CV studies of analogous dyes.[18]

We have recently shown that one of the key factors controlling the charge-recombination dynamics in molecular dye-sensitized nanocrystalline TiO_2 films is the spatial separation of the dye cation from the electrode surface.[17] More specifically we have demonstrated a linear correlation between the logarithm of the experimentally observed charge recombination half-time ($t_{50\%}$) and the spatial separation r of the molecular dye cation from the TiO_2 surface;[17] this is consistent with the expected exponential dependence of electron-transfer rate upon spatial separation ($k_{et} \propto e^{-\beta r}$, where β is the barrier height to electron tunneling and r is the spatial separation) from electron-tunneling theory.[27] Such data for the molecular sensitizers is shown in Figure 4 (points **A**–**E**) with the inclusion of the three supermolecular sensitizers **1**–**3** studied herein. Also included in the same plot is a supramolecular dye rotaxane **5**, based upon cyclodextrin encapsulated azobenzene chromophore and supermolecular dye **4** we have studied previously.[7,9] It is apparent that all

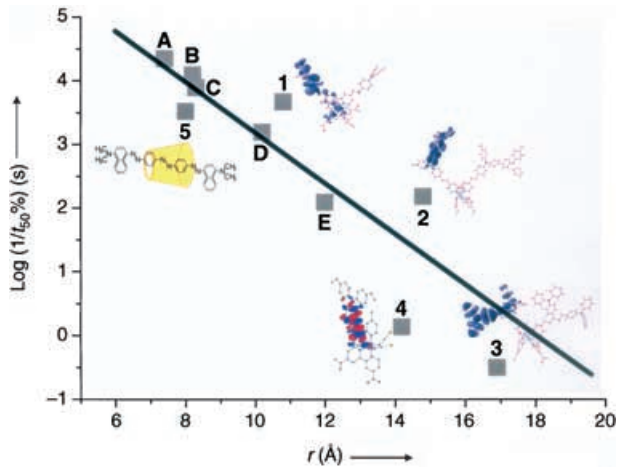

Figure 4. Plot of the logarithm of $1/t_{50\%}$ versus the spatial separation r of the dye cation from the TiO_2 surface for a series of dyes. Letters **A**–**E** represent series of molecular dyes studied previously:[17,29] **A** = [Ru(dcbpy)$_2$Cl$_2$], **B** = [Ru(dcbpy)$_2$(DTC)$_2$], **C** = [Ru(dcbpy)$_2$CN$_2$], **D** = [Ru(dcbpy)$_2$NCS$_2$], **E** = titanium phthalocyanine; DTC = $S_2CHN(C_2H_5)_2$. **1**–**3** are the supermolecular dyes studied herein, **4** is a supersensitizer dye[9] and **5** is a supramolecular dye,[7] both previously studied. The straight line is a linear fit to the experimental data following the theoretical treatment for electron-tunneling theory.[26] The slope of the line is indicative of the barrier height to tunneling $\beta = 0.95 \pm 0.2$ Å^{-1} as determined previously.[17] The influence of the free energy driving force ΔG has been factored into $t_{50\%}$ data shown here to give "free energy optimized" values as previously discussed.[17]

these five supermolecular dyes **1**–**5** lie reasonably well along the straight line, further indicating that the key parameter controlling the charge-recombination dynamics for the supersensitizers **1**–**4**, and also the supramolecular dye **5**, is the spatial separation of the dye cation from the surface of the electrode. Thus our quantitative relationship for the molecular dyes can be extended to the more complex supermolecular sensitizers. This is the first time such a quantitative relationship has been shown for nanocrystalline metal oxides sensitized with more complex supermolecular or supramolecular sensitizers.[27] Moreover we expect the present findings to have implications for the design of sensitizers for electronic applications such as dye-sensitized solar cells. A key requirement for the efficient operation of such devices is minimization of charge recombination. It is clear from Figure 4 that the more complex "supersensitizers" and in particular dyes **2**–**4**, exhibit considerably slower charge-recombination rates than the more simple molecular dyes. Our results suggest that to achieve a long-lived charge-separated life-time the sensitizer dye can be engineered such that the oxidizing equivalent "hole" resides further away from the TiO_2 surface after charge separation. As such, the use of sensitizer dyes with multistep charge-transfer cascades provides an attractive option for this purpose. Furthermore it is apparent from the data shown in Figure 2 that the temporal shape of the charge-recombination kinetics differs significantly between the three sensitizer dyes. The transient decays in Figure 4 were fitted to a stretched exponential function ($\Delta OD \propto \exp^{-(\omega\tau)}$) with $\alpha \approx 0.4$, $\alpha \approx 0.9$, and $\alpha = 1$ for dyes **1**, **2**, and **3**, respectively, as illustrated by the black lines in Figure 2. This shift is indicative of a transition from more inhomogeneous, transport-limited recombination dynamics to more homogeneous, interfacial electron-transfer-limited recombination dynamics as the spatial separation of the dye cation from the TiO_2 surface is increased, consistent with our previous observations.[7,17,18,28] We note that this shift has potentially important advantages for device optimization as the less dispersive (more mono-exponential) recombination dynamics observed for dyes **2** and **3** offer more potential for precise optimization of the kinetics and energetics of device function.

In summary we have reported a supermolecular dye-sensitized nanocrystalline TiO_2 film in which we are able to achieve a remarkably long-lived (4 s) charge-separated state. Our approach is based upon bifunctional sensitizer dyes. We find that the key parameter that controls charge transfer at the supermolecular-dye/TiO_2 interface is the spatial separation between the cation center of the dye and the electrode surface. More specifically the retardation in charge-recombination kinetics observed for dye **3** compared to dyes **2** and **1** results from a greater physical separation between the dye cation and TiO_2 film surface, which is consistent with the multistep translation of the oxidizing equivalent "hole" away from the surface, and in agreement with our DFT ab initio calculations. We note that the aryl-amine-based electron-donor groups used herein can be expected to electrically interface well with organic hole-transporting materials making our approach attractive for applications in solid-state dye-sensitized solar cells. Moreover, the wetting property of hole conductors may be improved as a result of the matching of the polarity at this interface. We further note that the hybrid integration of multifunctional materials with metal oxide surfaces and the ability of these structures to generate remarkably long-lived charge separation, may also provide a platform for the development of nanostructured optically driven data storage devices. The present findings show that the use of multifunctional dyes provides a versatile approach to the control of interfacial charge transfer.

Received: January 31, 2005
Revised: May 6, 2005
Published online: August 1, 2005

Keywords: dye sensitization · dyes/pigments · electron transfer · ruthenium · titanium oxide

[1] B. O'Regan, M. Grätzel, *Nature* **1991**, *353*, 737.
[2] U. Bach, D. Lupo, P. Compte, J. E. Moser, F. Weissortel, J. Salbeck, H. Spreitzer, M. Grätzel, *Nature* **1998**, *395*, 583.
[3] J. Krüger, R. Plass, L. Cevey, M. Piccirelli, M. Grätzel, U. Bach, *Appl. Phys. Lett.* **2001**, *79*, 2085.
[4] S. A. Haque, E. Palomares, H. Upadhyaya, L. Ottley, R. J. Potter, A. B. Holmes, J. R. Durrant, *Chem. Commun.* **2003**, 3008.
[5] E. Topoglidis, C. J. Campbell, E. Palomares, J. R. Durrant, *Chem. Commun.* **2002**, 1518.
[6] E. Palomares, R. Villar, J. R. Durrant, *Chem. Commun.* **2004**, 362.
[7] S. A. Haque, J. S. Park, M. Srinivasarao, J. R. Durrant, *Adv. Mater.* **2004**, *16*, 1177.
[8] K. Peter, H. Wietasch, B. Peng, M. Thelakkat, *Appl. Phys. A* **2004**, *79*, 65.
[9] N. Hirata, J. J. Lagref, E. J. Palomares, J. R. Durrant, M. K. Nazeeruddin, M. Grätzel, D. D. Censo, *Chem. Eur. J.* **2004**, *10*, 595.
[10] G. Will, J. Sotomayor, S. N. Rao, D. Fitzmaurice, *J. Mater. Chem.* **1999**, *9*, 2297.
[11] J. Sotomayer, G. Will, D. Fitzmaurice, *J. Mater. Chem.* **2000**, *10*, 685.
[12] A. Merrins, C. Kleverlaan, G. Will, S. N. Rao, F. Scandola, D. Fitzmaurice, *J. Phys. Chem. B* **2001**, *105*, 2998.
[13] A. Merrins, X. Marguerettaz, S. N. Rao, D. Fitzmaurice, *Chem. Eur. J.* **2001**, *7*, 1309.
[14] R. Argazzi, N. Y. M. Iha, H. Zabri, F. Odobel, C. A. Bignozzi, *Coord. Chem. Rev.* **2004**, *248*, 1299.
[15] H. Hofmeier, U. S. Schubert, *Chem. Soc. Rev.* **2004**, *33*, 373.
[16] V. Balzani, M. G. Lopez, J. F. Stoddart, *Acc. Chem. Res.* **1999**, *32*, 405.
[17] J. N. Clifford, E. Palomares, M. K. Nazeeruddin, M. Grätzel, J. Nelson, X. Li, N. Long, J. R. Durrant, *J. Am. Chem. Soc.* **2004**, *126*, 5225.
[18] J. N. Clifford, G. Yahioglu, L. R. Milgrom, J. R. Durrant, *Chem. Commun.* **2002**, 1260.
[19] K. Peter, M. Thelakkat, *Macromolecules* **2003**, *36*, 1779.
[20] S. A. Haque, Y. Tachibana, R. L. Willis, J. E. Moser, M. Grätzel, D. R. Klug, J. R. Durrant, *J. Phys. Chem. B* **2000**, *104*, 538.
[21] E. Palomares, J. N. Clifford, S. A. Haque, T. Lutz, J. R. Durrant, *J. Am. Chem. Soc.* **2003**, *125*, 475.
[22] S. A. Haque, T. Park, C. Xu, S. Koops, N. Schultes, R. J. Potter, A. B. Holmes, J. R. Durrant, *Adv. Funct. Mater.* **2004**, *14*, 435.
[23] G. Benko, J. Kallioinen, J. E. I. Korppi-Tommola, A. P. Yartsev, V. Sundstrom, *J. Am. Chem. Soc.* **2002**, *124*, 489.
[24] J. Ashbury, E. Hao, Y. Wang, H. N. Ghosh, T. Lian, *J. Phys. Chem. B* **2001**, *105*, 4545.

[25] Y. Tachibana, S. A. Haque, I. P. Mercer, J. E. Moser, D. R. Klug, J. R. Durrant, *J. Phys. Chem. B* **2001**, *105*, 7424.

[26] The spatial separation of the HOMO orbitals from the TiO_2 surface was determined by calculating the geometric distance between the carboxylate groups and each atom of the dye and by weighting this value with the square of the percentage contribution of each atom to the HOMO orbital. The spatial separation from the dye-cation moiety to the electrode surface was also calculated in three alternative ways: 1) by calculating the geometric distance between the carboxylate groups and the "edge" of the HOMO distribution, 2) by calculating the geometric distance between the Ti atom at surface of TiO_2 nanoparticle and each atom of the dye and by weighting this value with the square of the percentage HOMO orbital contribution, and 3) by calculating the geometric distance between the Ti atom at surface of TiO_2 nanoparticle and the "edge" of the HOMO distribution. All four methods yielded almost identical linear dependence of the charge-recombination rate upon spatial separation. We further note that the deviations of the data from the straight line fit in Figure 4 may be due to uncertainties in exact orientation of the anchored dyes on the TiO_2 electrode surface. We also note that for dye **3**, the DFT calculation was performed in a condition where the number of TPA units was 2. This therefore represents a lower limit for the extent of delocalization of the dye cation away from the ruthenium metal center and subsequently from the TiO_2 surface.

[27] D. S. Bendal in *Protein Electron Transfer, Outline of Theory of Protein Electron Transfer* (Eds.: C. C. Moser, P. L. Dutton), BIOS Scientific Publishers, Oxford, **1996**, chap. 1.

[28] J. Nelson, S. A. Haque, D. R. Klug, J. R. Durrant, *Phys. Rev. B* **2001**, *63*, 205321.

[29] E. Palomares, M. V. Martinez-Diaz, S. A. Haque, T. Torres, J. R. Durrant, *Chem. Commun.* **2004**, 2112.

